Interaction of atomic hydrogen with single-walled carbon nanotubes: A density functional theory study

Verónica Barone, Jochen Heyd, and Gustavo E. Scuseria
Department of Chemistry and Center for Biological and Environmental Nanotechnology, Rice University, Houston, Texas 77005

(Received 8 January 2004; accepted 21 January 2004)

We have studied the interaction of atomic hydrogen with (5,5) and (10,0) single-walled carbon nanotubes (SWNT) using density functional theory. These calculations use Gaussian orbitals and periodic boundary conditions. We compare results from the local spin density approximation, generalized gradient approximation (GGA), and hybrid density functionals. We have first kept the SWNT geometric structure fixed while a single H atom approaches the tube on top of a carbon atom. In that case, a weakly bound state with binding energies from -0.8 to -0.4 eV was found. Full geometry relaxation leads to a strong SWNT deformation, weakening the nearest C–C bonds and increasing the binding energy by about 1 eV. Full hydrogen coverage of the (5,5) SWNT converts this metallic nanotube into an insulator with a band gap of 3.4 eV for the GGA functional and 4.8 eV for the hybrid functional. Hybrid functionals perform similar to pure density functional theory functionals for the calculation of binding energies while band gaps critically depend on the functional choice. © *2004 American Institute of Physics.* [DOI: 10.1063/1.1668635]

INTRODUCTION

There is a growing interest in understanding the basics of the interaction between atomic or molecular hydrogen and single-walled carbon nanotubes (SWNT). One reason for this interest is the possibility of using SWNT for hydrogen storage. Many experimental[1–3] and theoretical[4–10] studies have been performed in order to understand the storage mechanism. However, the real storage capacity of these structures is still not clear. Experimental results on hydrogen storage are far from uniform and have not been independently reproduced.[11] The study of side-wall functionalization of SWNT has also attracted enormous attention lately because of its potential to separate metallic from semiconducting nanotubes, cut them, and even grow them in a selective way.[12,13]

Two different kinds of interactions can occur between hydrogen and a SWNT. One possibility is a physisorbed state where the molecular hydrogen does not dissociate and the interaction between the SWNT and the hydrogen molecule can be described as a van der Waals interaction. The other possibility is the dissociation of the hydrogen molecule with both atoms chemisorbed on the SWNT wall. Three interesting sites exist on which both types of adsorptions can occur: on top of a carbon atom, at the middle of a C–C bond, and at the center of a hexagon. Previous results identified carbon top sites, on both the inner and outer walls, as preferred sites for atomic hydrogen adsorption.[6]

In recent years, density functional theory (DFT) has been used to study the interaction of molecular and atomic hydrogen with SWNT. Both periodic boundary condition and cluster calculations have been performed using functionals based on the local spin density approximation (LSDA) and generalized gradient approximation (GGA).[4–10] Hybrid functionals, which contain a portion of the Hartree–Fock (HF) exchange, are in widespread use for calculations in molecular systems due to their higher accuracy compared to LSDA and GGA functionals.[14,15] However, in solid state calculations, hybrid functionals have not been commonly employed because of their high computational cost, as well as convergence problems arising when including a portion of HF exchange. These problems especially appear in metallic systems and small gap semiconductors. A recent alternative to conventional hybrid functionals are screened exchange hybrid functionals.[16] Such functionals make use of a screened Coulomb potential to reduce the spatial extent of the exact exchange interaction and provide results similar to traditional hybrid functionals while significantly reducing the computational effort.[17]

In this work, we study the interaction of atomic hydrogen with the (5,5) and (10,0) SWNT and present a systematic comparison between different functionals: LSDA, GGA, and screened exchange hybrid functionals. Such a study is presented for the first time utilizing hybrid functionals. We have chosen the (5,5) and (10,0) SWNT as model systems for metallic and semiconducting nanotubes since they have a unit cell of moderate size and have similar radii (approximately 4 Å).

In the following sections, we first outline the computational details of our calculations and then we present our results for potential energy surfaces, binding energies, and densities of states.

COMPUTATIONAL DETAILS

We have carried out all our calculations utilizing a development version of the Gaussian suite of programs.[18] Solid state calculations were performed using all-electron Gaussian basis sets and periodic boundary conditions. We have first optimized the isolated nanotube structures using the PBE[19]

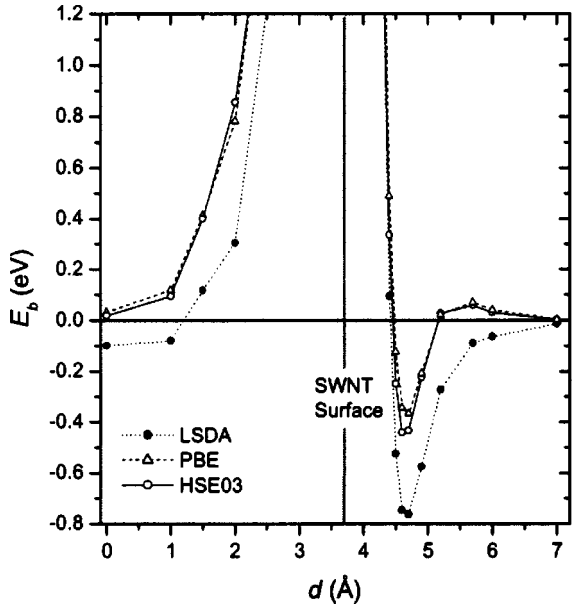

FIG. 1. Interaction of atomic H on top of a C atom with the (5,5) SWNT. We have kept the SWNT geometry fixed at the optimized PBE/6-31G* level structure for the isolated nanotube.

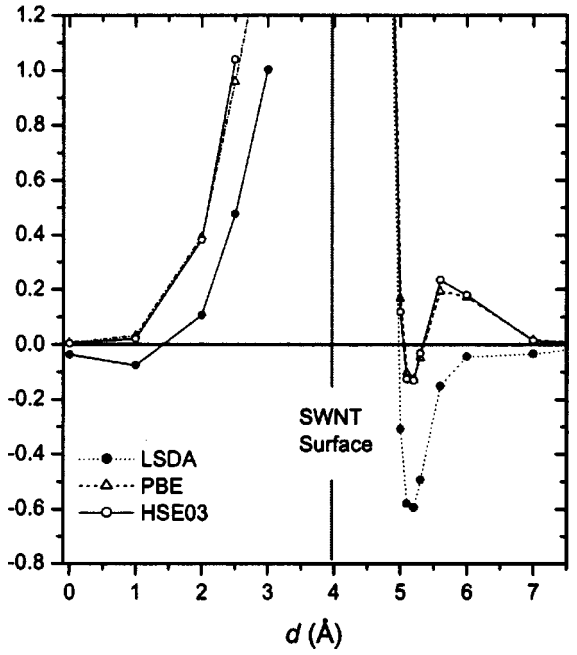

FIG. 2. Interaction of atomic H on top of a C atom with the (10,0) SWNT. We have kept the SWNT geometry fixed at the optimized PBE/6-31G* level structure for the isolated nanotube.

GGA functional and the 6-31G* basis set. Second, we have studied the interaction of atomic hydrogen with the undeformed (5,5) and (10,0) nanotubes using three different approaches: SVWN[20,21] (LSDA), PBE[19] (GGA), and HSE03 (Ref. 16) (screened exchange hybrid) functionals. We have employed the 6-31G basis set on carbon atoms $(3s2p)$ and the 6-31G** on hydrogen $(2s1p)$ for all energy calculations. In the case of single hydrogenation, the unit cell contained 21 atoms for the armchair and 41 atoms for the zigzag nanotube. A minimum number of 80 *k*-points was utilized for the first Brillouin zone integration. We have utilized the 6-31G basis set on carbon atoms and the 6-31G** on hydrogen for the calculation of the full geometry relaxation of the nanotube-hydrogen system and the full hydrogen coverage structures. For all open shell systems we have adopted an unrestricted Kohn–Sham approach.

All densities of states (DOS) were computed utilizing the 6-31G** basis set with both the PBE and HSE03 functionals.

RESULTS AND DISCUSSION

Single H atom and fixed SWNT geometry

In Figs. 1 and 2, we present the potential energy curve for the interaction between atomic hydrogen on top of a C atom and the (5,5) and (10,0) SWNT, respectively. In these calculations, we have kept the SWNT structure fixed while the H atom approaches from the center of the nanotube (inner wall) to several exohedral positions in the radial direction (outer wall), as shown in scheme I.

We have defined the binding energy in the usual way as

$$E_b = E(NT+H) - E(NT) - E(H), \tag{1}$$

where $E(NT+H)$ denotes the energy of the nanotube plus the H atom, $E(NT)$ is the energy of the bare nanotube, and $E(H)$ is the energy of the single H atom. In order to correct the potential energy surface for basis set superposition error (BSSE), we have utilized the counterpoise method.[22] To this end, we have evaluated the energy of the two different fragments, $E(NT)$ and $E(H)$, using the full basis set utilized to calculate the energy of the whole system, $E(NT+H)$. Within the definition given in Eq. (1), negative energies correspond to bound states. We observe a weak chemisorption in the outer wall for both nanotubes with all the studied functionals as shown in Figs. 1 and 2. The well-known trend that LSDA overestimates binding energies with respect to GGA and hybrid functionals can also be observed. In this case, PBE and HSE03 produce similar binding energies. In spite of both SWNT having similar radii (approximately 4 Å), the binding energy for the semiconducting nanotube is smaller than that of the metallic one: $E_b = -0.8$ eV (LSDA), -0.4 eV (PBE), and -0.5 eV (HSE03) for the metallic nanotube and $E_b = -0.6$ eV (LSDA), -0.1 eV (PBE), and -0.1 eV (HSE03) for the semiconducting SWNT. For both types of SWNT, a potential barrier separates the free H atom state from the bound state. This barrier is not present in the calculations performed using the LSDA approximation. LSDA produces a small physisorption in the interior of the nanotube

TABLE I. Binding energies and optimized geometrical parameters after full relaxation of the (5,5) and the (10,0) SWNT plus one H atom on top of the C atom utilizing different functionals. All energies are in eV and bond lengths in Å.

(5,5)		E_b	d_{C-H}	d_{C-C}	α_{CCH}	α_{CCC}
Fixed SWNT			1.250	1.435, 1.433		118.6, 119.5
	LSDA	−0.8				
	PBE	−0.4				
	HSE03	−0.5				
Full relaxation	LSDA	−2.2	1.115	1.545, 1.476	109.2, 110.8	106.4, 113.0
	PBE	−1.8	1.111	1.568, 1.493	109.1, 110.8	106.6, 112.8
	HSE03	−2.0	1.100	1.553, 1.482	109.3, 110.6	106.7, 112.6
	PBE0	−2.0	1.102	1.553, 1.484	109.4, 110.7	106.6, 112.6
Double unit cell full relaxation	LSDA	−2.1	1.117	1.522, 1.492	108.4, 107.7	109.8, 113.2
	PBE	−1.6	1.117	1.544, 1.511	108.5, 107.9	109.7, 113.1
	HSE03	−1.6	1.106	1.531, 1.500	108.7, 107.9	109.6, 112.9
(10,0)		E_b	d_{C-H}	d_{C-C}	α_{CCH}	α_{CCC}
			1.226	1.435, 1.427		117.6, 120.0
Fixed SWNT	LSDA	−0.6				
	PBE	−0.1				
	HSE03	−0.1				
Full relaxation	LSDA	−1.9	1.119	1.511, 1.484	108.5, 107.4	106.2, 113.5
	PBE	−1.5	1.116	1.534, 1.502	108.5, 107.5	106.4, 113.3
	HSE03	−1.5	1.085	1.522, 1.493	108.46, 107.6	106.3, 113.2

which is not present in the curve obtained with either the PBE or HSE03 functionals. Our LSDA results for the binding energies are in good agreement with those obtained by Arellano *et al.*[9] These authors also kept the SWNT geometry fixed but employed a plane-wave basis set, obtaining binding energies of about −1 eV.

For the sake of completeness, we have performed similar analyses to that of the ''on top'' site, with the H atom at the middle of a C–C bond and at the center of a hexagon for the (5,5) SWNT. In both cases, LSDA predicts a weak chemisorbed state at the exohedral position and a physisorbed state at the endohedral position, while no bound state is found with the PBE or HSE03 functionals.

Single H atom and full geometry optimization

The geometrical distortion of the nanotube structure due to the presence of a hydrogen atom is important and a full geometry optimization is required in order to obtain an accurate description of the binding energies of the system. We have performed a full relaxation structure optimization, considering the bound state found from our fixed SWNT geometry calculations as the initial geometry. Table I summarizes our results for binding energies and geometrical parameters calculated with LSDA, PBE, and HSE03 functionals. We have also considered a double unit cell in the case of the (5,5) SWNT. This unit cell contains 40 carbon atoms (instead of 20) and a single H atom. In this way, two consecutive hydrogen atoms (from different unit cells) are roughly at the same distance in both nanotubes.

We have defined the binding energy as in Eq. (1) and we have found the BSSE to be negligible. The full relaxation of the SWNT and hydrogen system gives a C–H bond length of about 1.11 Å and binding energies ranging from −2.2 (LSDA) to −1.5 eV (HSE03). Compared to the unperturbed geometries, it also produces a pronounced lengthening of the nearest C–C bonds (scheme II).

It is interesting to note that when considering the double sized unit cell for the (5,5) nanotube, the binding energies for both nanotubes are quite similar, in contrast with the single unit cell case. Our PBE result for E_b in the (10,0) SWNT (−1.5 eV) is smaller than the result obtained by Gülseren *et al.* using the GGA PW91 functional ($E_b \sim -2.3$ eV).[10] However, it is important to note that for the cases under consideration, binding energies obtained using the HSE03 functional are similar to the values obtained with the PBE functional. In contrast, bond lengths obtained with the PBE functional are longer by 0.01 to 0.03 Å than the corresponding HSE03 values.

We have also performed a full geometry optimization in the case of the (5,5) SWNT-H system with the standard hybrid PBE0[23] in order to compare these results with those obtained with HSE03. Table I shows an excellent agreement between both sets of results. Geometrical parameters and energies are almost identical while the computational cost for a single self-consistent-field (SCF) cycle of the conventional hybrid functional is about 4.5 times larger than in the case of the screened exchange functional.

TABLE II. Binding energies and selected geometrical parameters after full hydrogen coverage for the (5,5) and (10,0) SWNT. All energies are in eV and bond lengths in Å.

(5,5)	E_b	d_{C-H}	d_{C-C}	α_{CCH}	α_{CCC}
LSDA	−2.2	1.101	1.581, 1.550	94.7, 97.4	121.8, 112.7
PBE	−1.9	1.100	1.601, 1.573	94.8, 97.3	121.7, 112.9
HSE03	−1.9	1.090	1.587, 1.559	94.8, 97.3	121.7, 112.9
(10,0)	E_b	d_{C-H}	d_{C-C}	α_{CCH}	α_{CCC}
LSDA	−2.1	1.104	1.573, 1.556	93.3, 101.6	128.7, 114.1
PBE	−1.8	1.101	1.595, 1.583	93.6, 100.7	127.9, 114.5
HSE03	−1.8	1.090	1.568, 1.581	93.7, 100.5	127.8, 114.6

Full hydrogen coverage

Reported values of E_b for the exohedral full hydrogen coverage case range from −2.7 to −2.3 eV for the (10,0) SWNT and −2.9 eV for the (5,5) SWNT.[24,25] We have performed a full hydrogen coverage (scheme III)

optimization for the (5,5) and (10,0) SWNT. In this case, we have defined the mean binding energy, E_b, as an extension of the individual binding energy above

$$E_b = \frac{E(NT+nH) - E(NT) - nE(H)}{n}, \tag{2}$$

where n corresponds to the number of hydrogen atoms in the full coverage case [20 in the (5,5) and 40 in the (10,0) SWNT]. In Table II, we present selected geometrical parameters, as well as binding energies, for the LSDA, PBE, and HSE03 functionals. While the C–H bond length does not change dramatically in comparison with the single hydrogen case, the bond lengths of the two adjacent C–C bonds are closer to each other and become closer to a typical sp^3 C–C bond length. The binding energy of the full coverage system is slightly increased in comparison with the fully relaxed single hydrogen SWNT.

Densities of states

Interesting features related to the electronic structure of exohedral hydrogenation have been previously reported by Gülseren *et al.*[26] For instance, while full coverage hydrogenation of the metallic (9,0) SWNT produces an insulator material (energy gap of 2 eV), half coverage produces a metallic material with an unusually high density of states (DOS) at the Fermi level which has been speculated to lead to superconductivity.[26] We have studied the effect of hydrogenation on the DOS of the (5,5) SWNT for all cases considered in this work, i.e., fixed SWNT structure, fully relaxed structure, and full hydrogen coverage. We compare results between the PBE and HSE03 functionals. Changes in the DOS for the (5,5) SWNT after hydrogenation are more interesting to study than changes in the semiconducting nanotube since the (5,5) SWNT changes from a metallic to an insulator material. Covering the (10,0) SWNT with hydrogen only enlarges the existing energy gap.

In Figs. 3 and 4, we present the PBE and HSE03 densities of states of the (5,5) SWNT, respectively. Figures 3(a) and 4(a) present the DOS for the isolated (5,5) SWNT which is characterized by a small but nonzero density of states at the Fermi level, exhibiting a metallic behavior. Keeping the SWNT fixed and placing an H atom at the minimum of its potential energy surface, we note that the DOS shifts to zero around the Fermi level indicating the transition to a small gap semiconductor. The energy gap obtained with the HSE03 functional [Fig. 4(b)] is 2 times larger than the corresponding PBE value. However, both functionals predict the same trend. The presence of a single hydrogen atom opens an energy gap without taking into account any geometrical effects. By relaxing the SWNT geometry, this gap increases from 0.6 to 0.9 eV for PBE and from 1.1 to 1.4 eV for HSE03 [Figs. 3(c) and 4(c), respectively]. Full hydrogen coverage produces a sharp decay in the number of levels around the Fermi

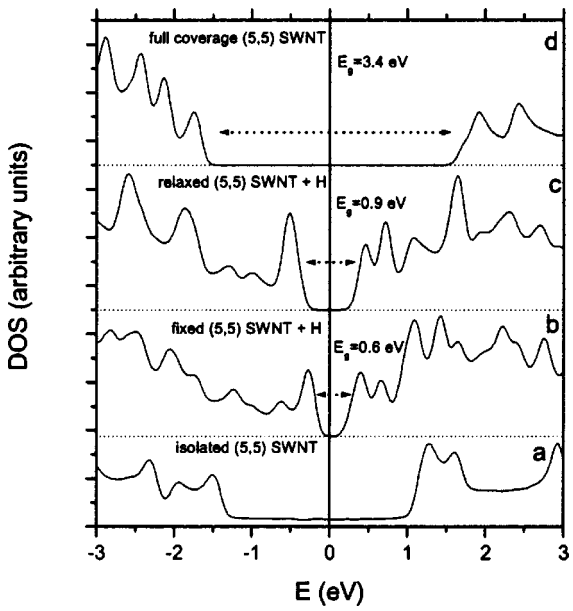

FIG. 3. Total DOS and band gaps (E_g) at the PBE/6-31G** level. (a) Isolated (5,5) SWNT; (b) isolated (5,5) structure and H atom at the bonded position; (c) relaxed structure of the (5,5) plus hydrogen system; (d) full hydrogen coverage case. Different DOS are shifted by a constant number (dotted horizontal line). The Fermi level is at zero (vertical line).

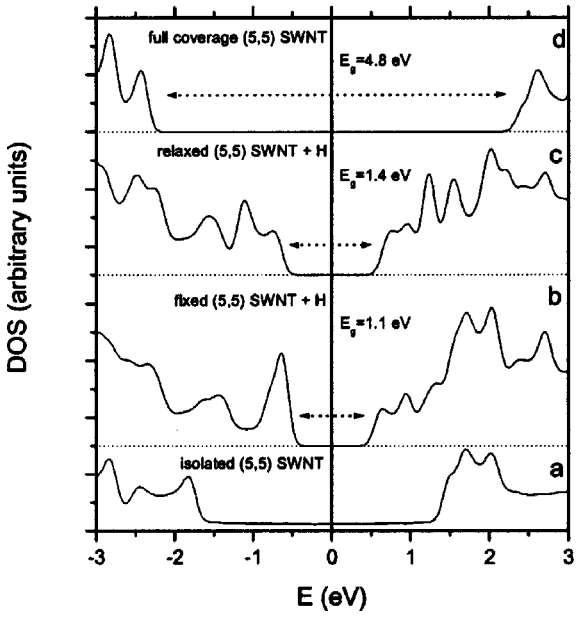

FIG. 4. Total DOS and band gaps (E_g) at the HSE03/6-31G** level. (a) Isolated (5,5) SWNT; (b) isolated (5,5) structure and H atom at the bonded position; (c) relaxed structure of the (5,5) plus hydrogen system; (d) full hydrogen coverage case. Different DOS are shifted by a constant number (dotted horizontal line). The Fermi level is at zero (vertical line).

energy, transforming this material in an insulator with an energy gap of about 3.4 eV for PBE and 4.8 eV for the HSE03. Experimental values for band gaps of SWNT after hydrogenation range from 1.9 to 4.4 eV.[27] However the pattern of hydrogenation obtained in the experiment is unclear (i.e., full coverage, half coverage, etc.). While the PBE results are fairly good for metallic systems, it has been shown that hybrid functionals perform much better for semiconducting and insulating systems.[28] This is mainly due to the inclusion of some Hartree–Fock exchange which tends to widen the energy gap, giving results in better agreement with experiment than those obtained with pure density functionals.

SUMMARY

This work presents a DFT study of the interaction between atomic hydrogen and (5,5) and (10,0) SWNT using different density functional approaches and including, for the first time, hybrid functionals. We have found a weak chemisorption in the outer wall without relaxing the SWNT geometric structure. A geometry relaxation produces a binding energy of about −1.5 eV. When the SWNT are completely covered by hydrogen, the binding energy is enlarged by about 0.3 eV. Screened hybrid functionals predict binding energies similar to the PBE values for the cases studied in this work. These results contrast with calculations in molecular systems where hybrid functionals give different results (usually performing better) for many thermodynamic properties.[14] This point deserves further investigation for the type of system under consideration in this paper.

From our results, we observe the high sensitivity of the electronic structure to the presence of a H atom. This sensitivity is clearly manifested in the total DOS and could be utilized to design custom electronic devices. In contrast to binding energies, the density of states is susceptible to the method employed. The HSE03 hybrid functional predicts larger band gaps than pure density functionals. Previous work has showed a general trend for pure functionals to underestimate band gaps.[28]

The screened hybrid HSE03 represents an attractive choice for including non-local exchange interactions without the significant computational effort of traditional hybrid functionals.

ACKNOWLEDGMENTS

This work was supported by the Nanoscale Science and Engineering Initiative of the National Science Foundation under NSF Award Number EEC-0118007, NSF-CHE9982156, and the Welch Foundation.

[1] C. Liu, Y. Y. Fan, M. Liu, H. T. Cong, H. M. Cheng, and M. S. Dresselhaus, Science **286**, 1127 (1999).
[2] B. N. Khare, M. Meyyappan, A. M. Cassell, C. V. Nguyen, and J. Han, Nano Lett. **2**, 73 (2002).
[3] K. A. Williams, B. K. Pradhan, P. C. Eklund, M. K. Kostov, and M. W. Cole, Phys. Rev. Lett. **88**, 165502 (2002).
[4] K. Tada, S. Furuya, and K. Watanabe, Phys. Rev. B **63**, 155405 (2001).
[5] J. Li, T. Furuta, H. Goto, T. Ohashi, Y. Fujiwara, and S. Yip, J. Chem. Phys. **119**, 2376 (2003).
[6] S. M. Lee, K. S. Park, Y. C. Choi *et al.*, Synth. Met. **113**, 209 (2000).
[7] Y. Okamoto and Y. Miyamoto, J. Phys. Chem. B **105**, 3470 (2001).
[8] C. W. Bauschlicher, Jr. and C. R. So, Nano Lett **2**, 337 (2002).
[9] J. S. Arellano, L. M. Molina, A. Rubio, M. J. López, and J. A. Alonso, J. Chem. Phys. **117**, 2281 (2002).
[10] O. Gülseren, T. Yildirim, and S. Ciraci, Phys. Rev. Lett. **87**, 116802 (2001).
[11] M. Hirscher, M. Becher, M. Haluska *et al.*, J. Alloys Compd. **654**, 330 (2002).
[12] Z. Gu, H. Peng, R. H. Hauge, R. E. Smalley, and J. L. Margrave, Nano Lett. **2**, 1009 (2002).
[13] M. S. Strano, C. A. Dyke, M. L. Usrey *et al.*, Science **301**, 1519 (2003).
[14] V. N. Staroverov, G. E. Scuseria, J. Tao, and J. P. Perdew, J. Chem. Phys. **119**, 12129 (2003).
[15] J. Tao, J. P. Perdew, V. N. Staroverov, and G. E. Scuseria, Phys. Rev. Lett. **91**, 146401 (2003).
[16] J. Heyd, G. E. Scuseria, and M. Ernzerhof, J. Chem. Phys. **118**, 8207 (2003).
[17] J. Heyd and G. E. Scuseria, J. Chem. Phys. (to be published).
[18] M. J. Frisch, G. W. Trucks, H. B. Schlegel *et al.*, Gaussian 03, Development Version (Rev. B.4), Gaussian Inc., Pittsburgh, PA, 2003.
[19] J. P. Perdew, K. Burke, and M. Ernzerhof, Phys. Rev. Lett. **77**, 3865 (1996).
[20] J. C. Slater, *Quantum Theory of Molecular and Solids. Vol. 4: The Self-Consistent Field for Molecular and Solids* (McGraw-Hill, New York, 1974).
[21] S. H. Vosko, L. Wilk, and M. Nusair, Can. J. Phys. **58**, 1200 (1980).
[22] S. F. Boys and F. Bernardi, Mol. Phys. **19**, 553 (1970).
[23] J. P. Perdew, K. Burke, and M. Ernzerhof, Phys. Rev. Lett. **77**, 3865 (1996).
[24] T. Yildirim, O. Gülseren, and S. Ciraci, Phys. Rev. B **64**, 075404 (2001).
[25] S. M. Lee, K. H. An, Y. H. Lee, G. Seifert, and T. Frauenheim, J. Am. Chem. Soc. **123**, 5059 (2001).
[26] O. Gülseren, T. Yildirim, and S. Ciraci, Phys. Rev. B **66**, 121401 (2002).
[27] K. S. Kim, D. J. Bae, J. R. Kim *et al.*, Adv. Mater. (Weinheim, Ger.) **14**, 1818 (2002).
[28] P. V. Avramov, K. N. Kudin, and G. E. Scuseria, Chem. Phys. Lett. **370**, 597 (2003).